



Incorporation of MgO into nitrogen-doped carbon to regulate adsorption for near-equilibrium isomerization of glucose into fructose in water

Qidong Hou^{a,1}, Mian Laiq Ur Rehman^{a,* ,1}, Xinyu Bai^a, Chao Xie^a, Ruite Lai^a, Hengli Qian^a, Tianliang Xia^a, Guanjie Yu^a, Yao Tang^a, Haijiao Xie^b, Meiting Ju^{a,*}

^a National & Local Joint Engineering Research Center of Biomass Resource Utilization, College of Environmental Science and Engineering, Nankai University, Tianjin 300350, China

^b Hangzhou Yanqu Information Technology Co., Ltd, Hangzhou City, Zhejiang Province 310003, China



ARTICLE INFO

Keywords:
Glucose
Isomerization
Fructose
Base
Adsorption

ABSTRACT

Glucose isomerization to fructose is an essential step for biomass valorization, but implementing this reaction via chemocatalysis suffers from low reaction efficiency and inferior catalyst reusability. Herein, MgO was incorporated into nitrogen-doped carbon via pyrolysis of ZIF-8 with MgCl₂ to synchronously enhance the catalytic performance and stability. The resultant MgO/NC-700 catalyst gave fructose yields of 42.9 % and 40.8 % at glucose loading of 10 and 20 wt%, respectively, approaching to the upper limit of reaction equilibrium. The average fructose productivity was 0.2267 mmol g⁻¹ h⁻¹, more than 2.29 times higher than the state-of-the-art heterogeneous catalysts. Moreover, the catalyst showed good stability and reusability without complicated regeneration steps. Isotope labelling study by NMR spectra revealed that the reaction is mainly proceeded via proton transfer mechanism. Both static adsorption experiment and DFT calculation indicated that the shift of reaction equilibrium towards fructose is due to the preferential adsorption of glucose.

1. Introduction

The transition away from fossil fuel resources toward ubiquitous lignocellulosic biomass resources is a promising approach to alleviate climate change [1]. This ambition stimulate the rapid development of biorefinery technology to convert biomass to commodity chemicals and transportation fuels, akin to the well-established petroleum refinery process [2]. In the search of economically viable and environmentally-friendly biorefinery routes, isomerization of aldoses into ketoses, in particular the isomerization of glucose to fructose has been highlighted as a pivotal reaction [3]. On the one hand, fructose is an important sweetening agent in food industry with the production of high fructose corn syrup up to 14 million metric tons per year. On the other hand, the use of fructose as starting material has shown great promise for the facile production of platform chemicals and biofuels, such as 5-hydroxymethylfurfural [4–7], lactic acid [8] and 5-ethoxymethylfurfural (EMF) [9]. Therefore, the effective transformation of glucose to fructose has been actively investigated in the past decades.

Enzyme-catalyzed glucose isomerization has been carried out on

industrial scale, as one of the greatest biocatalytic process [10]. This biotechnological process matches well with food industry due to the good safety of enzymes, and the cost can be compensated by the upper benefits of food production. Nevertheless, the large-scale application of glucose isomerase in biomass valorization to chemicals and fuels is unrealistic in view of its high cost and low lifetime [3]. Hence, acids and bases in both homogeneous and heterogeneous form have been thoroughly explored as catalyst to substitute enzymes [3,11–13]. Minority of Lewis acid catalysts, such as Sn-beta zeolite [14], single-unit-cell Sn-MFI zeolite (Sn-SPP) [15], H-USY zeolite [16], oxozirconium clusters on silica [17] and hafnium (Hf)-containing zeolites [18] showed outstanding catalytic performance in suitable solvents, with only isolated Sn embedded into a hydrophobic channel of beta zeolite being active in water [19]. The difficulty of catalyst preparation on large-scale, high cost, catalyst inactivation and the requirement of specific solvent environment [20,21] are major barriers for their industrial application.

In contrast to enzyme and Lewis acidic catalysts, basic catalysts have both much lower cost and less requirements for chemical environment. All kinds of Brønsted bases, including amines [22–25], alkali metal and

* Corresponding authors.

E-mail addresses: m.laeeq121@hotmail.com (M.L.U. Rehman), jumeit@nankai.edu.cn (M. Ju).

¹ These authors contributed equally to this work.

alkaline-earth metal based oxides [26–29], hydroxides [8,24,30–34], phosphates [35,36], carbonates [37] and composites [13,28,38–43] exhibited notable catalytic performance. For both homogeneous and heterogeneous base catalysts, the fructose yields in aqueous solution are limited to 30–40 % [3]. Recently, significantly elevated fructose yields of 52 % in 1-butanol [32] and 56 % in ethanol [31] over Mg-Al hydrotalcite (HT) catalyst have been achieved. However, the displacement of water with organic solvents require complex separation and purification process, with the increase of solvent cost and safety risks. Likewise, the addition of neutral salt improved the fructose yield from 30 % to 41 % over polystyrene-supported organic bases catalyst [44] at the expense of complicated downstream processes with secondary pollution. Considering industrial applications, the heterogeneous catalyst should be cost-effective, environmentally friendly, active and recyclable in pure water [36].

Although apparent fructose yield has been widely used to evaluate catalytic activity, it can't accurately represent actual reaction efficiency of a whole catalytic system [28]. Since the reaction are restricted by reaction equilibrium and side-reaction, the decrease of fructose selectivity along with the increase of glucose conversion is unavoidable [3]. Thus, the room for improvement of reaction efficiency via further improving fructose yields is marginal. Currently, the isomerization reaction is generally conducted with glucose loading no more than 10 wt %, and the upper fructose yields are usually achieved at glucose loading around 1 wt% [15,16,18,31]. In this view, performing the reaction at high substrate loading is of great importance for the substantive improvement of reaction efficiency. Once the catalytic systems are capable to convert high loading of glucose to fructose directly, the high-concentration products could be readily subjected to separation, purification or downstream process, thus greatly reducing the process cost. Comprehensively considering solvent and catalyst, the actual reaction efficiency should be assessed by the average productivity of the whole catalytic system [2].

The stability and reusability of catalyst should also be emphasized during design stage for commercial viability [36,45]. Unfortunately, the deactivation of acidic, basic catalysts and isomerase has been universally observed [36,46–49]. Heterogeneous base catalysts face multiple deactivation modes, such as structural collapse, species deposition and loss of active sites [27,28,47,50,51]. The deposited organic species could be erased via calcination from inorganic materials to recover their activity, but the organic-containing materials loss activity irreversibly during reaction. The loss of active sites doubtlessly leads to irreversible catalyst deactivation. By far, only a few of heterogeneous base catalysts could maintain catalytic activity in recycling experiment with indispensable catalyst regeneration process. For instance, the regeneration of HT require intricate steps, including energy-intensive calcination and restoration of layered structure via the memory effect in ammonium carbonate solution [31]. Our recent work exhibited that the composition, structure and activity of barium modified hydroxyapatite could be recovered after calcination due to the effective inhibition of metal leaching, but this method need to displace water with ethanol as solvent [36]. The avoidance of multistep operations for catalyst regeneration would be highly rewarding.

To realize efficient isomerization of high-loading glucose into fructose in the medium of water and synchronously achieve facile reuse of catalyst, MgO/nitrogen-doped carbon material was prepared from ZIF-8 and MgCl₂ using two-step pyrolysis process. The nitrogen-doped carbon trended to distribute on the surface as protective layer with MgO being incorporated into porous structure, as is different from previous supported catalysts. The catalytic performance for glucose isomerization exceeded previously reported catalysts with improved stability and reusability. Based on catalytic performance and catalyst characterizations, we reveal that the improvement of reaction efficiency and the shift of reaction equilibrium towards fructose is likely due to the preferential adsorption of glucose.

2. Experimental section

Metal-organic framework (MOF) ZIF-8 was prepared according to previously reported method [52], as precursor of porous nitrogen-doped carbon materials with highly dispersed N species. First, 2-methylimidazole (29.15 g/L, weight of 2-methylimidazole) and Zn(NO₃)₂·6H₂O (12.75 g/L weight of 2-methylimidazole were dissolved in deionized water (1 L) to prepare the corresponding aqueous solutions, respectively. The two aqueous solutions were blended with sufficient stirring for 2 h and then setting overnight. The resulting white precipitate was gathered by centrifugation and washed several times with water and ethanol, alternately. The final solid was dried at 80 °C in oven.

100 mg of ZIF-8 and 359.35 mg of MgCl₂·6H₂O were added into 20 mL of ethanol and dispersed via sonication for 10 min. Subsequently, ethanol was evaporated from the mixture by heating under controlled temperature with stirring and then dried at 80 °C overnight. The resultant white powder was first calcination at 300 °C (heating rate, 5 °C min⁻¹) for 5 h in a nitrogen flow. After thorough washing using a water-ethanol mixture, the dried powders (80 °C) were subjected to secondary high-temperature annealing (550 °C, 700 °C and 800 °C, respectively; heating rate of 2 °C min⁻¹) for 5 h in a nitrogen flow. The final product obtained was named as MgO/NC-550, MgO/NC-700 and MgO/NC-800, respectively. Details for catalyst characterizations, evaluation of catalytic performance and theory calculation are provided in the supporting information.

3. Results and discussion

Elemental analysis (Table 1) showed that MgO/NC-550 and MgO/NC-700 have comparable C and N content, while MgO/NC-800 has obviously lower C and N content. The N/C ratio decreased continuously with the increase of pyrolysis temperature, suggesting that suitable temperature is crucial for the maintenance of nitrogen-doped carbon structure. The successful loading of Mg species onto the nitrogen-doped carbon was verified by ICP-OES analysis. For MgO/NC-700 and MgO/NC-800, most of Zn species were removed during the calcining process. XPS analysis (Fig. 1a, 2) showed that the surface Mg content in MgO/NC-700 is comparable to that in MgO/NC-550, while the surface N content in the former is more than two times higher than the latter. The surface and bulk N/Mg atomic ratios for MgO/NC-550 were approximately equal (0.282 and 0.257, respectively), suggesting that the elemental distributions in MgO/NC-550 is uniform. In contrast, the surface N/Mg atomic ratio (0.671) in MgO/NC-700 was distinctly higher than the bulk N/Mg atomic ratio. In view of the accompanied C element, we deduced that Mg species is incorporated into nitrogen-doped carbon structure that potentially serves as a protective layer.

As exhibited in XRD patterns (Fig. 1b), MgO/NC-550, MgO/NC-700 and MgO/NC-800 all showed characteristic peaks of crystalline MgO at 37.0°, 43.0°, 62.4°, 74.7° and 78.6°, corresponding to the (111), (200), (220), (311) and (222) lattice planes, respectively [40]. The intensity of peaks in MgO/NC-700 were larger than those of MgO/NC-550 and MgO/NC-800, suggesting the higher crystallinity of MgO in MgO/NC-700. Raman spectra (Fig. 1c) showed two broad bands centered at about 1586 and 1323 cm⁻¹ resulted from the graphitized carbon (G band) and disordered carbon (D band) species, respectively [53]. The intensity ratio of D band to G band for MgO/NC-550, MgO/NC-700 and MgO/NC-800 were calculated to be 1.34, 1.14 and 1.06, respectively, indicating that evaluated temperature is helpful for the graphitization of materials. In FTIR spectra (Fig. S2), the OH peak in MgO/NC-700 was obviously lower than the other two materials.

SEM images (Fig. S3) showed that MgO/NC-700 is composed of irregular granule of several microns. High-resolution TEM images showed the presence of small lattice fringes with spacings of 0.210 nm corresponded to (200) lattice plane of MgO [54], as is consistent with the XRD analysis. N₂ adsorption-desorption isotherms showed that the specific surface area (Table 2) of MgO/NC-700 and MgO/NC-800 are 5.8

Table 1
Surface and bulk element composition of catalysts.

Samples	Elemental content (wt% ^a)			Metal content (wt% ^b)		Surface element composition (at% ^c)				
	C	N	H	Mg	Zn	C	O	N	Mg	Zn
MgO/NC-550	9.66	5.18	1.80	34.57	13.01	43.91	33.26	4.19	14.87	3.77
MgO/NC-700	11.15	4.90	0.89	39.56	3.03	38.89	36.81	9.42	14.04	0.84
MgO/NC-800	5.29	0.86	0.35	46.24	3.75	34.24	35.57	4.88	24.98	0.33

^a Elemental contents determined by elemental analysis.

^b Bulk metal content determined by ICP-OES.

^c at%: atomic percent determined by XPS analysis.

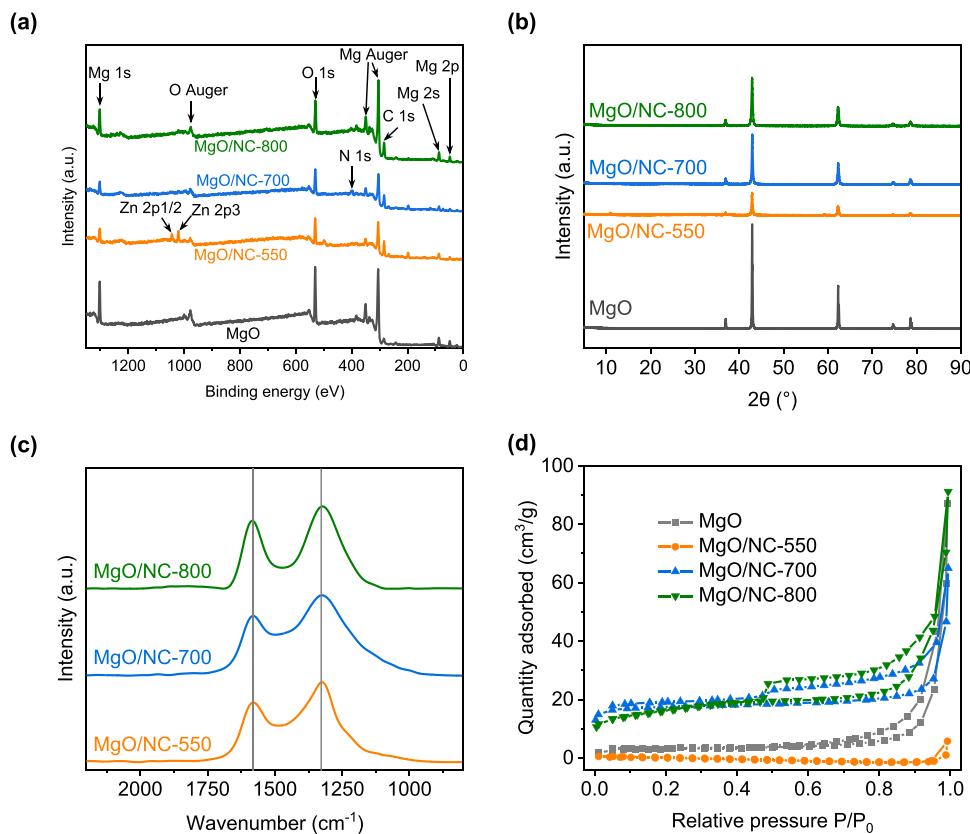


Fig. 1. (a) XPS survey spectra, (b) XRD patterns, (c) Raman spectra and (d) N_2 adsorption-desorption isotherms of MgO, MgO/NC-550, MgO/NC-700 and MgO/NC-800.

and 4.9 times higher than that of MgO. The remarkable improvement of surface area may enhance mass-transfer between catalyst and reactant, as is beneficial to the improvement of catalytic performance. CO_2 temperature programming desorption ($\text{CO}_2\text{-TPD}$) curve (Fig. S5) exhibited a strong peak ranged from 400° to 750°C and a weak peak centered at about 150°C , verifying the presence of strong basic sites and weak basic sites, respectively.

In summary, a composite composed of MgO and nitrogen-doped carbon is successfully constructed by co-pyrolysis of ZIF-8 with MgCl_2 at suitable calcination temperature (700°C). Previous study showed that pyrolysis temperature makes a decisive contribution to the structure of carbon materials [55]. The MgO/NC-550 obtained at lower temperature (550°C) has low specific surface area and homogenous elemental distribution. In MgO/NC-700, highly crystallized MgO is incorporated into the porous structure with partial exposed lattice plane, while nitrogen-doped carbon tends to concentrate upon surface to function as a protective layer. In contrast, the MgO/NC-800 obtained at higher temperature (800°C) show decreased C and N contents with reduced specific surface area. These results indicated that nitrogen-doped carbon and MgO are gradually formed and synchronously assembled into

porous composite during calcination, but excessive temperature would damage the nitrogen-doped carbon structure probably owing to the decomposition of N-containing groups. For traditional MgO/carbon materials, small amount of MgO is generally supported on the surface of composite. By contrast, in MgO/NC-700 large amount of MgO is incorporated into the porous nitrogen-doped carbon structure with tight interfacial contact, as is beneficial to the material's stability. Moreover, the formation of nitrogen-doped carbon may facilitate the preferential adsorption of glucose, since nitrogen-containing functional groups could enhance the adsorption of aldehydes [56].

The catalytic isomerization of glucose toward fructose over different materials (Fig. 3) was performed at 90°C using pure water as solvent with catalyst loading of 2 wt% and glucose loading of 5 wt%. The fructose yield-time curves for MgO/NC-550, MgO/NC-700 and MgO/NC-800 catalysts all exhibited semblable volcano trend. The increase of calcination temperature of catalysts seems to be favorable for the improvement of glucose conversion rate but with the expense of reduced fructose selectivity. The highest fructose yields over these three catalysts was 36.1 %, 39.9 % and 37.2 %, respectively. For comparison, the catalytic performance of ZIF-8, ZIF-8 calcined at 700°C for 5 h (NC-700),

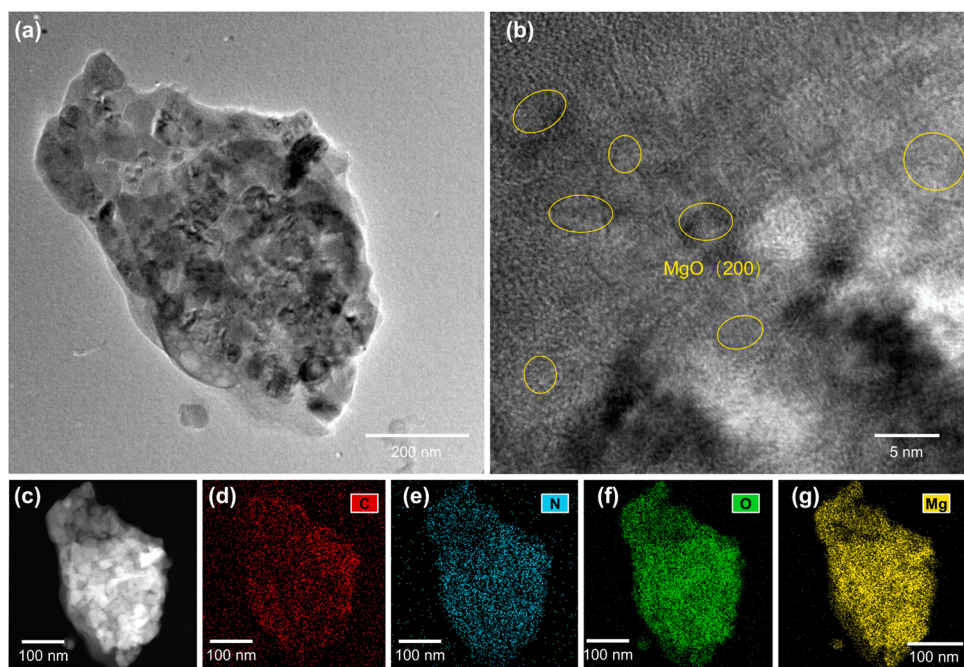


Fig. 2. TEM images and element mapping of MgO/NC-700.

Table 2
Textural properties of catalysts.

Samples	Surface area ($\text{m}^2 \text{ g}^{-1}$)	Pore volume ($\text{cm}^3 \text{ g}^{-1}$)	Average pore Diameter (nm)
MgO	11.6	0.034	32.8
MgO/NC-550	0.78	—	—
MgO/NC-700	67.4	0.078	16.2
MgO/NC-800	56.6	0.067	12.8

commercial MgO, 700 °C calcined MgO (MgO-700) were also tested under the same reaction condition. Both ZIF-8 and NC-700 exhibited relatively poor performance. Commercial MgO gave fructose yield of 31.1 % but the selectivity was relatively low, as is comparable to the performance of various MgO materials reported in previous studies [26–28,39,57]. The calcination of MgO leaded to slightly elevated glucose conversion with lower fructose yield and selectivity. The MgO/NC catalysts, in particular MgO/NC-700 showed significantly higher fructose yields and selectivities than MgO, ZIF-8 and NC-700 materials.

Both advantageous and disadvantageous influences of organic solvents have been observed in previous studies [31,32,36,48,58]. Herein, the MgO/NC-700 catalyst (Fig. 4a) showed poor performance for glucose conversion when using methanol, ethanol or butanol as solvents. When butanol/water or ethanol/water mixtures were used as reaction medium, the increase of water proportion leaded to obviously improvement of fructose yield. These results demonstrated water is most suitable solvent for glucose isomerization over this catalyst, as is significant for commercial viability.

The reusability of MgO/NC-550 and MgO/NC-700 was evaluated in four run's recycling experiment. The recovery rates of MgO/NC-550 and MgO/NC-700 after reaction were estimated to be 96.8 % and 98.3 %, respectively. For MgO/NC-550 (Fig. 4b), the fructose yield decreased gradually from 36.1 % to 32.5 % at the fourth run. In contrast, the catalytic activity of MgO/NC-700 (Fig. 4c) was well preserved, with fructose yield reducing slightly from 39.9 % to 38.3 %. For MgO based materials, including MgO [51], MgO-doped ordered mesoporous carbon

(OMC@MgO) [39] and MgO-biochar [40], catalyst inactivation were commonly observed owing to gradual dissolution of MgO by acidic products and carbonaceous deposits. Although several studies showed that the catalytic activity of MgO [26], MgO/carbon nanocomposite [59] and macroporous niobium phosphate-supported MgO (MgO/NbO) [28] could be well maintained, the regeneration of catalysts via calcination are indispensable after each recycling. Unlike these catalysts, the MgO/NC-700 catalyst is readily reused without energy-consuming calcination step. In addition, after treating with HCl solution, MgO/NC-700 still gave fructose yield of 34.3 % (Fig. 4d). ICP-OES analysis showed that the Mg contents in HCl treated MgO/NC-700 is 38.05 %, corresponding to a Mg leaching rate (3.8 %) (Table S1) that is even lower than those under reaction conditions from majority of MgO-based materials (Table S2). This result suggested that MgO/NC-700 is resistant to acidic environment to some extent, as is superior to previously developed MgO-based catalysts [28,40,59].

The above results showed MgO/NC-700 has both good catalytic activity and reusability. Thus, the reaction conditions are further optimized for this catalyst. As shown in Fig. 5, MgO/NC-70 gave fructose yield up to 38.7 % even at catalyst loading of 5 mg (2 wt% with respect to the glucose loading) that is considerably lower than the effective catalyst dosage used in previous reports [27,39,48]. Both glucose conversion and fructose yield increased with catalyst loading increases from 5 to 50 mg, and then decreased as catalyst loading was further improved to 150 mg. At appropriate catalyst loading of 50 mg, fructose yield up to 41.5 % was reached. Except for catalyst loading of 5 mg, the fructose selectivity decreased with the increase of catalyst loading, as is same with the trend of MgO catalyst [26].

Since low dosage of MgO/NC-700 is capable to convert glucose effectively, we further test if it could tolerate high-concentration glucose. The optimal fructose yield at glucose loading of 1 wt% (Fig. 6) was lower than that at glucose loading of 5 wt%, probably due to the aggravated side-reaction by superfluous catalyst. At glucose loading of 10 wt%, MgO/NC-700 gave fructose yield 42.9 % with selectivity of 81.4 %. With the further addition of glucose loading to 15 wt% and 20 wt%, just 100 mg of MgO/NC-700 catalyst still gave fructose yields 41.2 % and 40.8 % with selectivity of 73.6 % and 74.9 %, respectively. These results demonstrated that MgO/NC-700 is capable to convert high-concentration glucose. In previous studies, remarkable decrease of

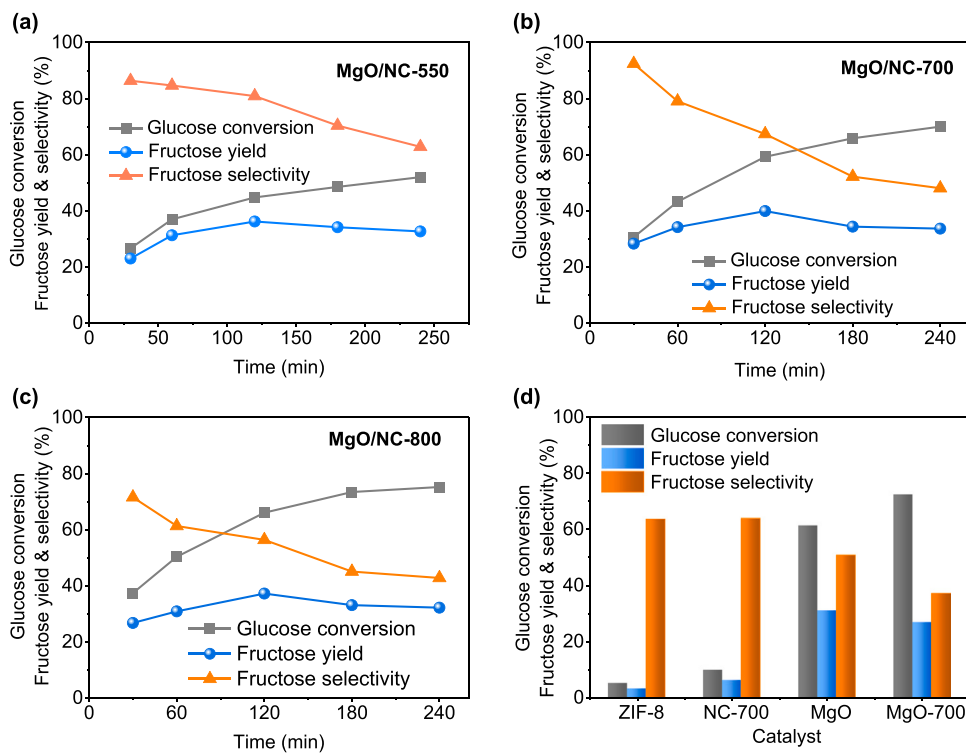


Fig. 3. Catalyst performance of (a) MgO/NC-550, (b) MgO/NC-700 and (c) MgO/NC-800. Reaction conditions: glucose (0.25 g), catalysts (100 mg), water (5 mL), temperature (90°C). (d) Performance of ZIF-8, NC-700, MgO and MgO-700 under the same condition (reaction time of 2 h if unspecified).

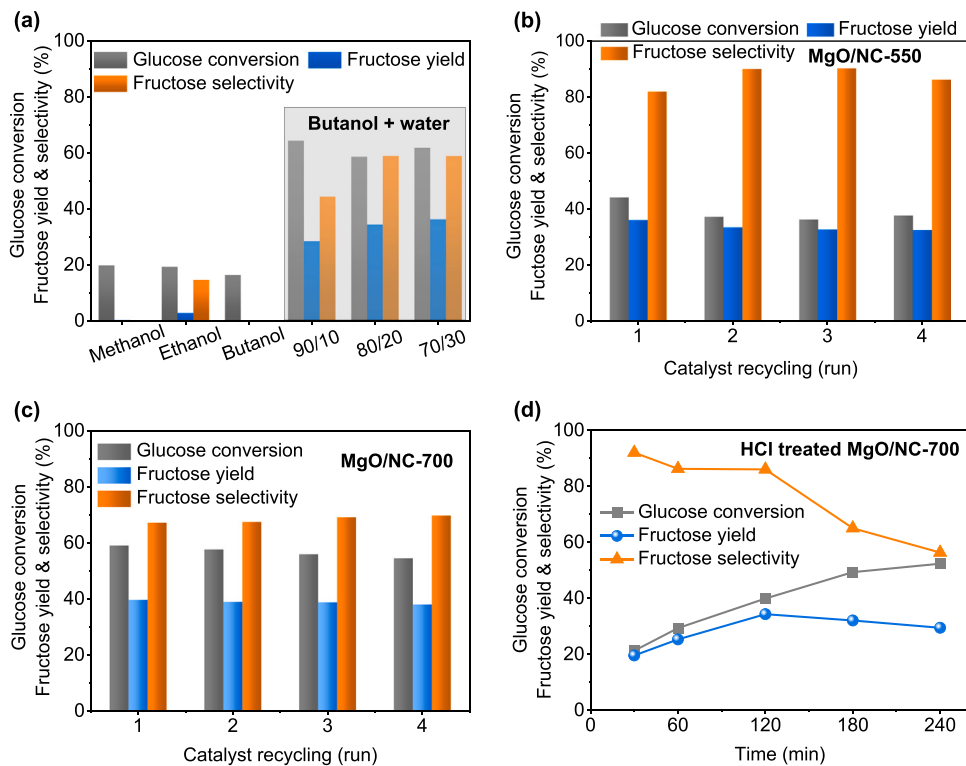


Fig. 4. (a) Influence of solvents on the catalyst performance of MgO/NC-700. Reuse of MgO/NC-550 (b) and MgO/NC-700 (c) in recycling experiment. (d) Catalytic performance of HCl treated MgO/NC-700 catalyst (treating the catalyst with 2 M HCl with stirring for 2 h). Reaction conditions: glucose (0.25 g), catalysts (100 mg), water (5 mL), temperature (90°C).

fructose yield with the increase of glucose loading have been extensively observed for various catalytic systems [32,39]. To the best of knowledge, glucose isomerization has been seldom performed at such a high

substrate loading. The good performance at both low catalyst dosage and high substrate loading demonstrated the great catalytic capacity of MgO/NC-700 catalyst.

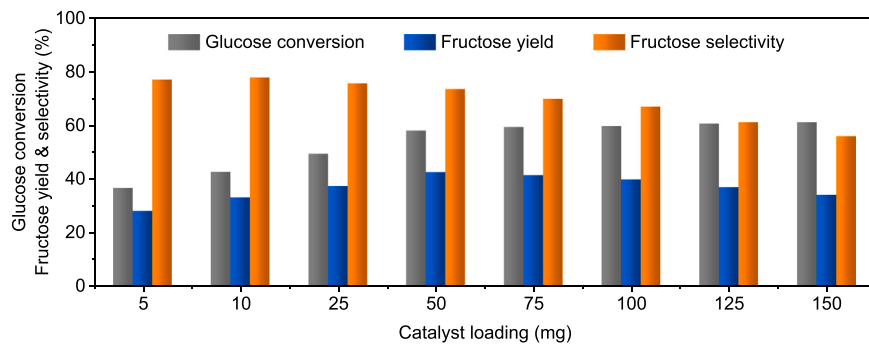


Fig. 5. Influence of catalyst loading on glucose isomerization to fructose. Reaction conditions: glucose (0.25 g), water (5 mL), temperature (90°C), reaction time (2 h).

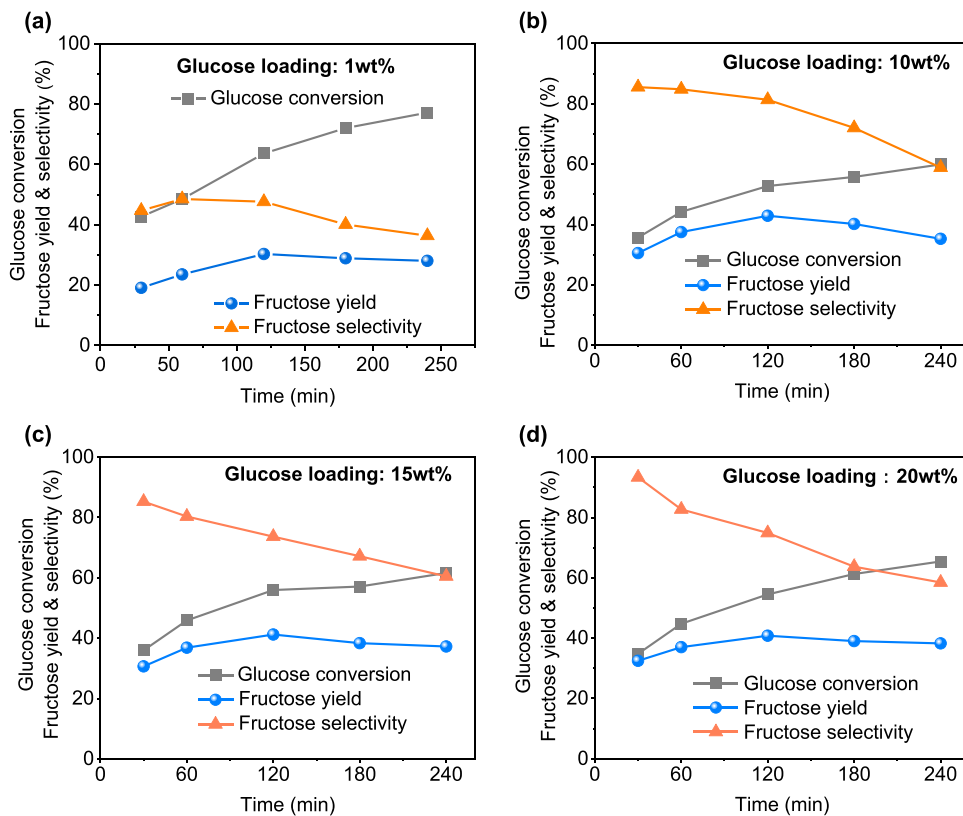


Fig. 6. Influence of glucose loading on the performance of the MgO/NC-700 catalyst. Reaction conditions: glucose, water (5 mL), catalyst loading (100 mg), temperature (90°C).

We also compared the performance of MgO/NC-700 to various catalysts previously designed for this reaction. MgO supported on different materials [28,39,40,59] had been widely investigated for this reaction, but the maximal fructose yields (24.6–34.58 %) were not substantially improved in relative to individual MgO (33.4 %), likely due to the compromise between improved accessibility and reduced loading of MgO [26,27]. When the reaction was performed in water, the fructose yield obtained with MgO/NC-700, approaching to the upper limit of enzymatic catalysis, is better than or comparable to the state-of-the-art catalysts regardless of reaction conditions, indicating that the reaction equilibrium shifts slightly towards fructose. For unambiguous comparison of reaction efficiency, the average productivity of catalytic systems is defined as the average fructose yield per weight of catalytic system per unit of time at their correspondingly optimal conditions. Accordingly, the productivity of MgO/NC-700 based catalytic system (Fig. 7) is calculated to be $0.2267 \text{ mmol g}^{-1} \text{ h}^{-1}$, at least 2.29 times higher than

the state-of-the-art heterogeneous catalytic systems. The productivity of Sn-SPP [15], H-USY zeolite [16], Sn-beta [14] and chromium hydroxide/MIL-101(Cr) MOF composite (MIL-101-[GLY]) based catalytic system are low since their superior yields (41–65 %) were achieved at low glucose loading with long reaction time. As a benchmark catalyst, HT has been extensively tested in different solvents. Up to now, the highest productivity ($0.0567 \text{ mmol g}^{-1} \text{ h}^{-1}$) of HT was obtained in butanol, since this combination gave high yield at glucose loading up to 10 wt% [32]. Barium modified hydroxyapatite (Ba/HAP) in ethanol also delivered relatively high productivity owing to the high substrate loading and relatively low reaction time [36]. Among previously reported catalysts, one kind of MgO attained the highest productivity ($0.0990 \text{ mmol g}^{-1} \text{ h}^{-1}$) owing to the short reaction time with maximal fructose yield of 33.4 % [26,27], while other kind of MgO materials can't give such good performance [39]. When only considering the weight of catalyst, the maximal average productivity of MgO (the

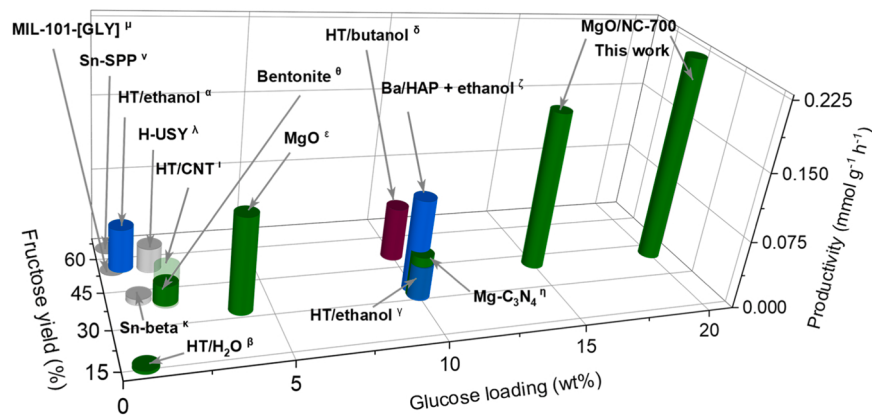


Fig. 7. Comparison of performance with previously reported catalytic systems. α , ref. [31]; β , ref. [31]; γ , ref. [32]; δ , ref. [32]; ε , ref. [61]; ζ , ref. [36]; η , ref. [48]; θ , ref. [62]; ι , ref. [57]; κ , ref. [46]; λ , ref. [16]; μ , ref. [63], ν , ref. [15]: detailed reaction condition are given in Table S3.

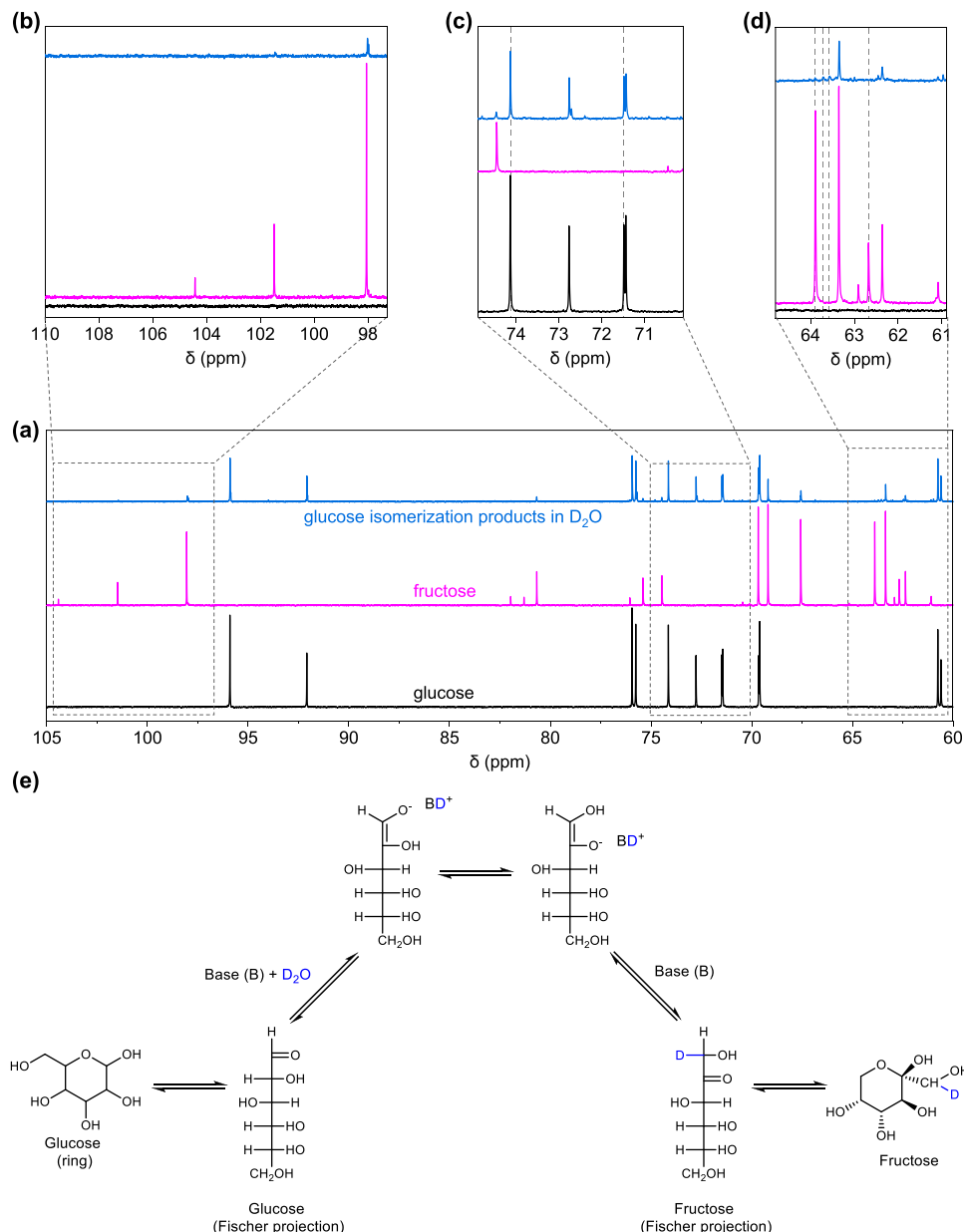


Fig. 8. (a-d) ^{13}C NMR spectra of glucose, fructose, and glucose isomerization products in D_2O (Reaction condition: 250 mg of glucose, 5 mL of D_2O , 100 mg of MgO/NC-700 catalyst, 90°C, 2 h). (e) The mechanism of glucose isomerization to fructose via proton transfer.

fructose yield per weight of catalyst per unit of time at their correspondingly optimal conditions) was even higher than MgO/NC-700. Taken together, the incorporation of MgO into nitrogen-doped carbon slightly reduce the reaction rate of glucose isomerization, but significantly improve selectivity, ultimately leading to higher yields and improved reaction efficiency. Homogeneous catalytic systems, such as triethylamine [22,23] and meglumine [24] gave fructose yields of 31 % and 35 % in reaction time (7–30 min) considerably shorter than heterogeneous catalytic systems [60], but they suffered from recycling challenges. Therefore, we quantificationally revealed that the MgO/NC-700 based catalytic system has superior productivity compared with other catalysts, regardless of the differences of reaction conditions. Combining with the aforementioned characterizations, these results demonstrated that incorporating MgO into porous nitrogen-doped carbon structure could greatly improve the catalytic performance.

To explore the reaction mechanism, a labelling study was conducted in deuterium oxide (D_2O) and the product distribution were investigated with high-resolution ^{13}C NMR spectra. The ^{13}C NMR spectra of MgO/NC-700 catalyzed glucose isomerization products in D_2O (Fig. 8) showed the characteristic peaks of both fructose and glucose, confirming the occurrence of glucose isomerization to fructose. The unlabeled fructose exhibited ^{13}C resonance at $\delta = 63.9$ and 62.7 ppm, corresponding to the C1 position of β -pyranose and β -furanose, respectively. For MgO/NC-700 catalyzed glucose isomerization products in deuterium oxide (D_2O), these two signals was greatly attenuated with the appearance of a new triplet peak ($\delta = 63.9, 63.7, 63.5$ ppm), demonstrating that the resultant fructose is deuterated at the C1 position [64]. The C2 carbon in unlabeled glucose showed two singlets at $\delta = 74.1$ ppm (β -pyranose) and 71.4 ppm (α -pyranose), respectively. These two peaks in glucose-2-D appear as low-intensity triplets due to

nuclear Overhauser enhancement by the deuterium atom at the C2 position [32]. These two peaks were reserved in the MgO/NC-700 catalyzed glucose isomerization products in D_2O , indicating that direct exchange of deuterium/hydrogen between glucose and D_2O is limited under the tested condition. The 1H NMR spectra (Fig. S7) of unlabeled fructose shows two strong peaks at $\delta = 3.45$ due to the presence of a hydrogen atom in the C1 position. These peaks disappeared in the glucose isomerization products in D_2O , again proving that the formed fructose is deuterated at the C1 position. These results indicated that the glucose-fructose isomerization is mainly proceeded via a proton-transfer mechanism (Lobry de Bruyn-Alberda van Ekenstein mechanism) (Fig. 6e) [65].

To reveal the reason for the slight shift of reaction equilibrium, static adsorption of fructose and glucose over MgO and MgO/NC-700 was tested. As discussed above, MgO/NC-700 has much higher specific surface area and pore volume than MgO. The glucose adsorption amount (Fig. 9a) on MgO/NC-700 catalyst was 1.52 times higher than that of fructose. In contrast, fructose adsorption amount on MgO was considerably higher than glucose. DFT theoretical calculations were performed to give deep insight on the inherent reasons for the different adsorption preference of MgO and MgO/NC-700. The MgO surface with (200) lattice plane was modeled with a 15 Å vacuum in the z direction to separate the slabs. A simplified model of MgO/NC-700 was constructed by considering the C, N, Mg contents and MgO (200) lattice plane, and assuming nitrogen-doped carbon is present on the surface of MgO. As shown in Fig. 9b, the glucose adsorption energy (E_{ads}) on MgO was 0.10 eV higher than that of fructose, suggesting that MgO will adsorb fructose preferentially. In contrast, the glucose adsorption energy on MgO/NC-700 was 0.06 eV lower than that of fructose, indicating that MgO/NC-700 could adsorb larger amount of glucose than fructose. The differences of adsorption capability indicated by theoretical calculations

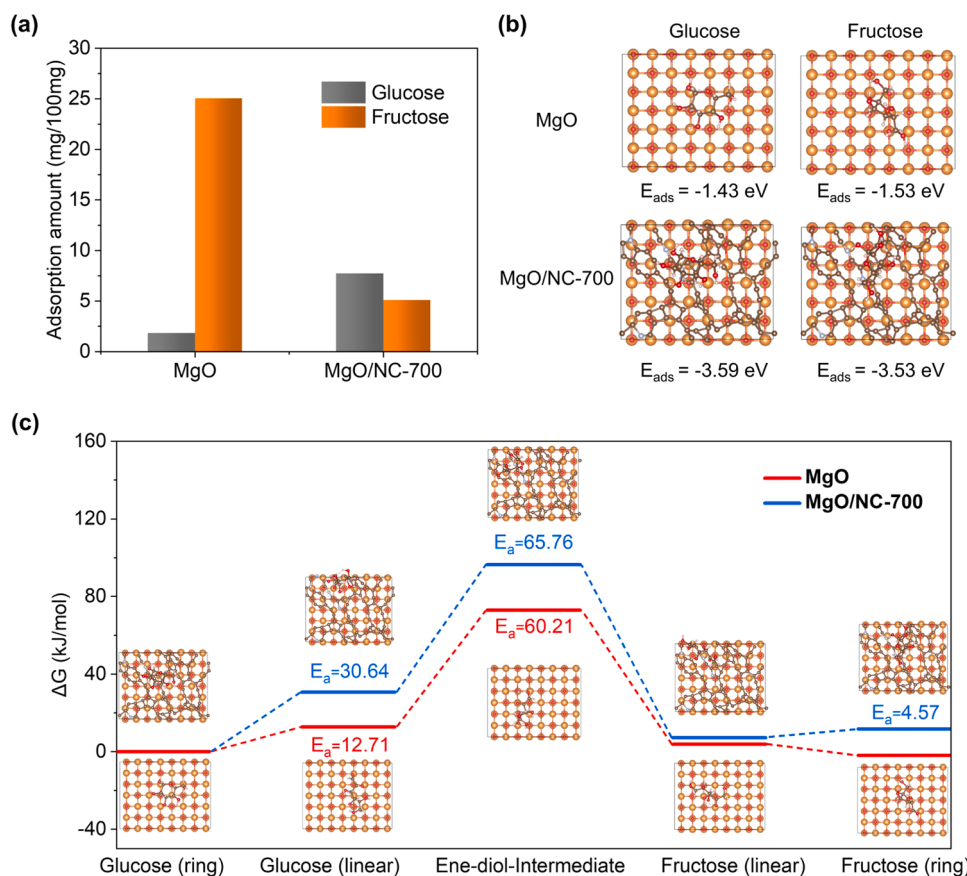


Fig. 9. (a) Static adsorption of fructose and glucose onto MgO and MgO/NC-700 (Reaction condition: 50 mg of glucose, 5 mL of water, 100 mg of catalyst, 25°C, 24 h). (b) calculated glucose and fructose adsorption energy on MgO and MgO/NC-700. (c) Comparison of the reaction energy barrier over MgO and MgO/NC-700.

are basically consistent with the experimentally determined adsorption data. As discussed above, MgO and MgO/NC-700 had same (200) lattice plane, but in the latter material MgO is incorporated into the porous nitrogen-doped carbon structure with partial exposed lattice plane and remarkably improved specific surface area. Previous study showed that the introduction of N into carbon material could obviously enhance the adsorption of acetaldehyde [56]. Thus, we deduced that different adsorptive ability between MgO/NC-700 with MgO is mainly resulted from the improved specific surface area and the presence of N containing groups.

Based on the reaction pathway demonstrated by NMR study, the reaction energy barriers of different steps, including ring opening of cyclic glucose to linear form, transformation of linear glucose to enediol-intermediate, transformation of ene-diol-intermediate to linear fructose and transformation of linear fructose to cyclic fructose on the MgO and MgO/NC-700 catalysts were estimated. The results indicated that transformation of linear glucose to ene-diol-intermediate is the rate-determining step. The reaction energy barrier (65.76 kJ/mol) of the rate-determining step over MgO/NC-700 was slightly higher than that (60.21 kJ/mol) over MgO (Fig. 9c), as is contrary to the trend of fructose yields but is in accordance with the lower reaction rate over MgO/NC-700 than MgO. This counterintuitive phenomenon was probably due to the compromise of the reduced exposure of MgO (200) lattice plane as available active center with the improvement of mass transfer. It should be pointed out that the advantage of MgO/NC-700 over MgO is the shift of reaction equilibrium toward fructose to reach higher equilibrium yield, instead of accelerate reaction rate. Thus, the different catalytic performance of MgO/NC-700 and MgO matched well with their adsorption performance. The accumulation of fructose on MgO could not only impede the proceeding of glucose isomerization, but also exacerbate fructose degradation. Thus, we attributed the slight shift of reaction equilibrium to fructose to the preferential adsorption of glucose onto the MgO/NC-700 catalyst.

Combining the results of material characterization with catalytic performance, we conclude the improved performance of MgO/NC-700 compared with MgO is reached via the following mechanism (Fig. 10). First, the combination of MgO with nitrogen-doped carbon could regulate the adsorption behavior of glucose and fructose. Second, the preferential adsorption of glucose could not only reduce side-reactions, but also shift the reaction equilibrium towards fructose. As a compromise of slight reduced reaction rate and significantly improve selectivity, the

final yield and actual reaction efficiency was remarkably improved. Besides, both the reduction of side-reactions and the protection effect of nitrogen-doped carbon on MgO would improve its stability and reusability.

In summary, we demonstrated that incorporating MgO into nitrogen-doped carbon structure is effective for the substantive improvement of catalytic performance and reusability. The precise regulation of glucose and fructose adsorption/desorption on heterogeneous catalyst would further improve the fructose yield via shifting the reaction equilibrium. The catalyst design strategy present here may be instructive for further development of active and robust solid base catalysts. However, the fructose selectivity obtained with MgO/NC-700 is still inferior to glucose isomerase, as a major disadvantage for its application in industrial production. Endeavors are still on the way to construct highly selective catalysts analogous to enzymes to avoid side-reactions. According to the deep understanding on glucose isomerase, it's possible to design heterogeneous catalysts with well-defined active sites and tunable acid-base strength to speed up glucose isomerization at near-ambient temperature. In addition, the chemical microenvironment around active sites should be precisely tuned to regulate the directed adsorption and desorption of reactants and products. Thus, owing to the mild reaction condition and rapid desorption of products, the side-reactions might be greatly reduced.

4. Conclusions

In this study, MgO/nitrogen-doped carbon were designed as catalyst for the isomerization of glucose to fructose. A series of characterizations confirmed that the composite structure of MgO and nitrogen-doped carbon with relatively high surface area was successfully constructed. MgO/NC-700 exhibited excellent catalytic performance in the medium of water. With glucose loading as high as 10 wt% and 20 wt%, the MgO/NC-700 catalyst still gave the fructose yields of 42.9 % and 40.8 %, approaching to the upper limit of enzymatic isomerization conducted in water. Significantly, the average productivity was calculated to be $0.2267 \text{ mmol g}^{-1} \text{ h}^{-1}$, at least 2.29 times higher than the state-of-the-art heterogeneous catalytic systems. Moreover, the catalytic activity can be well maintained in recycling experiment without complicated catalyst regeneration steps. We inferred that the selective adsorption of glucose may boost the slight shift of reaction equilibrium towards fructose. The NMR analysis revealed that the glucose isomerization is mainly

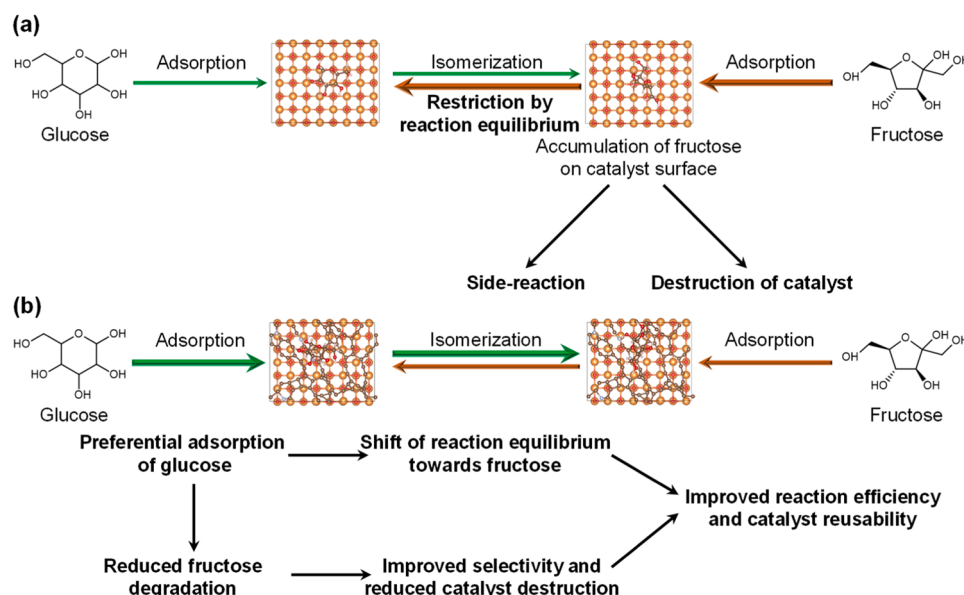


Fig. 10. Proposed mechanism for the improved catalytic performance and reusability of MgO/NC-700 (b) compared with MgO (a).

proceeded via proton transfer mechanism. Achieving superior reaction in pure water and good catalyst reusability, this study would greatly expedite the low-cost and highly efficient production of fructose from glucose.

CRediT authorship contribution statement

Qidong Hou: Conceptualization, Design of materials, Characterization, Writing – review & editing and Supervision; **Mian Laiq Ur Rehman:** Preparation of materials, Evaluation of catalytic performance; **Xinyu Bai:** Preparation of materials, Investigation; **Chao Xie:** Investigation; **Ruite Lai:** Methodology; **Hengli Qian:** Methodology; **Tianliang Xia:** Investigation; **Guanjie Yu:** Investigation; **Yao Tang:** Investigation; **Haijiao Xie:** Software for theory calculation; **Meiting Ju:** Supervision.

Declaration of Competing Interest

The authors declare no conflict of interest.

Data availability

Data will be made available on request.

Acknowledgements

This work was supported by the National Natural Science Foundation of China (22208169, 21878163).

Appendix A. Supporting information

Supplementary data associated with this article can be found in the online version at [doi:10.1016/j.apcatb.2023.123443](https://doi.org/10.1016/j.apcatb.2023.123443).

References

- [1] W. Deng, Y. Feng, J. Fu, H. Guo, Y. Guo, B. Han, Z. Jiang, L. Kong, C. Li, H. Liu, P.T. T. Nguyen, P. Ren, F. Wang, S. Wang, Y. Wang, Y. Wong, S.S. Wong, K. Yan, N. Yan, X. Yang, Y. Zhang, Z. Zhang, X. Zeng, H. Zhou, Catalytic conversion of lignocellulosic biomass into chemicals and fuels, *Green. Energy Environ.* 8 (2023) 10–114.
- [2] Q. Hou, X. Qi, M. Zhen, H. Qian, Y. Nie, C. Bai, S. Zhang, X. Bai, M. Ju, Biorefinery roadmap based on catalytic production and upgrading 5-hydroxymethylfurfural, *Green. Chem.* 23 (2021) 119–231.
- [3] I. Delidovich, Toward understanding base-catalyzed isomerization of saccharides, *ACS Catal.* (2023) 2250–2267.
- [4] Q. Hou, W. Li, M. Ju, L. Liu, Y. Chen, Q. Yang, One-pot synthesis of sulfonated graphene oxide for efficient conversion of fructose into HMF, *RSC Adv.* 6 (2016) 104016–104024.
- [5] Q. Hou, W. Li, M. Zhen, L. Liu, Y. Chen, Q. Yang, F. Huang, S. Zhang, M. Ju, An ionic liquid–organic solvent biphasic system for efficient production of 5-hydroxymethylfurfural from carbohydrates at high concentrations, *RSC Adv.* 7 (2017) 47288–47296.
- [6] C. Bai, Q. Hou, X. Bai, Y. Nie, H. Qian, M. Zhen, M. Ju, Conversion of glucose to 5-hydroxymethylfurfural at high substrate loading: effect of catalyst and solvent on the stability of 5-hydroxymethylfurfural, *Energy Fuels* 34 (2020) 16240–16249.
- [7] Q. Hou, C. Bai, X. Bai, H. Qian, Y. Nie, T. Xia, R. Lai, G. Yu, M.L.U. Rehman, M. Ju, Roles of ball milling pretreatment and titanyl sulfate in the synthesis of 5-hydroxymethylfurfural from cellulose, *ACS Sustain. Chem. Eng.* 10 (2022) 1205–1213.
- [8] X. Zhao, Z. Zhou, H. Luo, Y. Zhang, W. Liu, G. Miao, L. Zhu, L. Kong, S. Li, Y. Sun, γ -Valerolactone-introduced controlled-isomerization of glucose for lactic acid production over an Sn-Beta catalyst, *Green. Chem.* 23 (2021) 2634–2639.
- [9] Y. Nie, Q. Hou, H. Qian, X. Bai, T. Xia, R. Lai, G. Yu, M.L.U. Rehman, M. Ju, Synthesis of mesoporous sulfonated carbon from chicken bones to boost rapid conversion of 5-hydroxymethylfurfural and carbohydrates to 5-ethoxymethylfurfural, *Renew. Energy* 192 (2022) 279–288.
- [10] S. Wu, R. Snajdrova, J.C. Moore, K. Baldenius, U.T. Bornscheuer, Biocatalysis: enzymatic synthesis for industrial applications, *Angew. Chem. Int. Ed.* 60 (2021) 88–119.
- [11] I. Delidovich, R. Palkovits, Catalytic isomerization of biomass-derived aldoses: a review, *ChemSusChem* 9 (2016) 547–561.
- [12] H. Li, S. Yang, S. Saravanamurugan, A. Riisager, Glucose isomerization by enzymes and chemo-catalysts: status and current advances, *ACS Catal.* 7 (2017) 3010–3029.
- [13] P. Zhu, S. Meier, S. Saravanamurugan, A. Riisager, Modification of commercial Y zeolites by alkaline-treatment for improved performance in the isomerization of glucose to fructose, *Mol. Catal.* 510 (2021), 111686.
- [14] M. Moliner, Y. Roman-Leshkov, M.E. Davis, Tin-containing zeolites are highly active catalysts for the isomerization of glucose in water, *Proc. Natl. Acad. Sci. USA* (2010) 6164–6168.
- [15] L. Ren, Q. Guo, P. Kumar, M. Orazov, D. Xu, S.M. Alhassan, K.A. Mkhyoyan, M. E. Davis, M. Tsapatsis, Self-pillared, single-unit-cell Sn-MFI zeolite nanosheets and their use for glucose and lactose isomerization, *Angew. Chem. Int. Ed.* 54 (2015) 10848–10851.
- [16] S. Shunmugavel, M. Paniagua, J.A. Melero, A. Riisager, Efficient isomerization of glucose to fructose over zeolites in consecutive reactions in alcohol and aqueous media, *J. Am. Chem. Soc.* (2013) 5246–5249.
- [17] C.D. Malonzo, S.M. Shaker, L. Ren, S.D. Prinslow, A.E. Platero-Prats, L. C. Gallington, J. Borycz, A.B. Thompson, T.C. Wang, O.K. Farha, J.T. Hupp, C. C. Lu, K.W. Chapman, J.C. Myers, R.L. Penn, L. Gagliardi, M. Tsapatsis, A. Stein, Thermal stabilization of metal–organic framework-derived single-site catalytic clusters through nanocasting, *J. Am. Chem. Soc.* 138 (2016) 2739–2748.
- [18] L. Botti, S.A. Kondrat, R. Navar, D. Padovan, J.S. Martinez-Espin, S. Meier, C. Hammond, Solvent-activated hafnium-containing zeolites enable selective and continuous glucose–fructose isomerisation, *Angew. Chem. Int. Ed.* 59 (2020) 20017–20023.
- [19] P. Zhu, H. Li, A. Riisager, Sn-Beta catalyzed transformations of sugars—advances in catalyst and applications, *Catalysts* 12 (2022) 405.
- [20] Q.D. Hou, M.N. Zhen, W.Z. Li, L. Liu, J.P. Liu, S.Q. Zhang, Y.F. Nie, C.Y.L. Bai, X. Y. Bai, M.T. Ju, Efficient catalytic conversion of glucose into 5-hydroxymethylfurfural by aluminum oxide in ionic liquid, *Appl. Catal. B-Environ.* 253 (2019) 1–10.
- [21] Q. Hou, M. Zhen, L. Liu, Y. Chen, F. Huang, S. Zhang, W. Li, M. Ju, Tin phosphate as a heterogeneous catalyst for efficient dehydration of glucose into 5-hydroxymethylfurfural in ionic liquid, *Appl. Catal. B: Environ.* 224 (2018) 183–193.
- [22] J.M. Carraher, C.N. Fleitman, J.-P. Tessonniere, Kinetic and mechanistic study of glucose isomerization using homogeneous organic Brønsted base catalysts in water, *ACS Catal.* 5 (2015) 3162–3173.
- [23] C. Liu, J.M. Carraher, J.L. Swedberg, C.R. Herndon, C.N. Fleitman, J.-P. Tessonniere, Selective base-catalyzed isomerization of glucose to fructose, *ACS Catal.* 4 (2014) 4295–4298.
- [24] S.S. Chen, D.C.W. Tsang, J.-P. Tessonniere, Comparative investigation of homogeneous and heterogeneous Brønsted base catalysts for the isomerization of glucose to fructose in aqueous media, *Appl. Catal. B: Environ.* 261 (2020), 118126.
- [25] Q. Yang, T. Runge, Polyethylenimines as homogeneous and heterogeneous catalysts for glucose isomerization, *ACS Sustain. Chem. Eng.* 4 (2016) 6951–6961.
- [26] A.A. Marianou, C.M. Michailof, A. Pineda, E.F. Iliopoulos, K.S. Triantafyllidis, A. A. Lappas, Glucose to fructose isomerization in aqueous media over homogeneous and heterogeneous catalysts, *ChemCatChem* 8 (2016) 1100–1110.
- [27] A.A. Marianou, C.M. Michailof, D.K. Ipsakis, S.A. Karakoulia, K.G. Kalogiannis, H. Yiannoulaikis, K.S. Triantafyllidis, A.A. Lappas, Isomerization of glucose into fructose over natural and synthetic MgO Catalysts, *ACS Sustain. Chem. Eng.* 6 (2018) 16459–16470.
- [28] D.-M. Gao, Y.-B. Shen, B. Zhao, Q. Liu, K. Nakanishi, J. Chen, K. Kanamori, H. Wu, Z. He, M. Zeng, H. Liu, Macroporous niobium phosphate-supported magnesia catalysts for isomerization of glucose-to-fructose, *ACS Sustain. Chem. Eng.* 7 (2019) 8512–8521.
- [29] J. Ohyama, Y. Zhang, J. Ito, A. Satsuma, Glucose isomerization using alkali metal and alkaline earth metal titanates, *ChemCatChem* 9 (2017) 2864–2868.
- [30] I. Delidovich, R. Palkovits, Catalytic activity and stability of hydrophobic Mg–Al hydrotalcites in the continuous aqueous-phase isomerization of glucose into fructose, *Catal. Sci. Technol.* 4 (2014) 4322–4329.
- [31] M. Yabushita, N. Shibayama, K. Nakajima, A. Fukuoka, Selective glucose-to-fructose isomerization in ethanol catalyzed by hydrotalcites, *ACS Catal.* 9 (2019) 2101–2109.
- [32] P.P. Upare, A. Chamas, J.H. Lee, J.C. Kim, S.K. Kwak, Y.K. Hwang, D.W. Hwang, Highly efficient hydrotalcite/1-butanol catalytic system for the production of the high-yield fructose crystal from glucose, *ACS Catal.* 10 (2020) 1388–1396.
- [33] S. Park, D. Kwon, J.Y. Kang, J.C. Jung, Influence of the preparation method on the catalytic activity of Mg/Al hydrotalcites as solid base catalysts, *Green. Energy Environ.* 4 (2019) 287–292.
- [34] J. Kang, G. Lee, Y.W. Suh, J. Jung, Effect of Mg/Al atomic ratio of Mg–Al hydrotalcites on their catalytic properties for the isomerization of glucose to fructose, *J. Nanosci. Nanotechnol.* 17 (2017) 8242–8247.
- [35] R.D. Patria, M.K. Islam, L. Luo, S.-Y. Leu, S. Varjani, Y. Xu, J.W.-C. Wong, J. Zhao, Hydroxyapatite-based catalysts derived from food waste digestate for efficient glucose isomerization to fructose, *Green. Synth. Catal.* 2 (2021) 356–361.
- [36] Q. Hou, M. Laiq Ur Rehman, X. Bai, H. Qian, R. Lai, T. Xia, G. Yu, Y. Tang, H. Xie, M. Ju, Enhancing the reusability of hydroxyapatite by barium modification for efficient isomerization of glucose to fructose in ethanol, *Fuel* 338 (2023), 127308.
- [37] V. Toussaint, I. Delidovich, Revealing the contributions of homogeneous and heterogeneous catalysis to isomerization of d-glucose into d-fructose in the presence of basic salts with low solubility, *Catal. Sci. Technol.* 12 (2022) 4118–4127.
- [38] F. Shen, J. Fu, X. Zhang, X. Qi, Crab shell-derived lotus rootlike porous carbon for high efficiency isomerization of glucose to fructose under mild conditions, *ACS Sustain. Chem. Eng.* 7 (2019) 4466–4472.
- [39] J. Fu, F. Shen, X. Liu, X. Qi, Synthesis of MgO-doped ordered mesoporous carbons by Mg²⁺–tannin coordination for efficient isomerization of glucose to fructose, *Green. Energy Environ.* (2021).

- [40] S.S. Chen, Y. Cao, D.C.W. Tsang, J.-P. Tessonnier, J. Shang, D. Hou, Z. Shen, S. Zhang, Y.S. Ok, K.C.W. Wu, Effective dispersion of MgO nanostructure on biochar support as a basic catalyst for glucose isomerization, *ACS Sustain. Chem. Eng.* 8 (2020) 6990–7001.
- [41] H. Zhang, H. Zhao, S. Zhai, R. Zhao, J. Wang, X. Cheng, H.S. Shiran, S. Larter, M. G. Kibria, J. Hu, Electron-enriched Lewis acid-base sites on red carbon nitride for simultaneous hydrogen production and glucose isomerization, *Appl. Catal. B: Environ.* 316 (2022), 121647.
- [42] J. Wang, H. Zhao, B. Zhu, S. Larter, S. Cao, J. Yu, M.G. Kibria, J. Hu, Solar-driven glucose isomerization into fructose via transient Lewis acid-base active sites, *ACS Catal.* (2021) 12170–12178.
- [43] S. E, C. Jin, J. Liu, L. Yang, M. Yang, E. Xu, K. Wang, K. Sheng, X. Zhang, Engineering functional hydrochar based catalyst with corn stover and model components for efficient glucose isomerization, *Energy* 249 (2022), 123668.
- [44] Q. Yang, W. Lan, T. Runge, Salt-promoted glucose aqueous isomerization catalyzed by heterogeneous organic base, *ACS Sustain. Chem. Eng.* 4 (2016) 4850–4858.
- [45] A.J. Martín, S. Mitchell, C. Mondelli, S. Jaydev, J. Pérez-Ramírez, Unifying views on catalyst deactivation, *Nat. Catal.* 5 (2022) 854–866.
- [46] Q. Guo, L. Ren, S.M. Alhassan, M. Tsapatsis, Glucose isomerization in dioxane/water with Sn- β catalyst: improved catalyst stability and use for HMF production, *Chem. Commun.* 55 (2019) 14942–14945.
- [47] I. Graça, M.C. Bacariza, A. Fernandes, D. Chadwick, Desilicated NaY zeolites impregnated with magnesium as catalysts for glucose isomerisation into fructose, *Appl. Catal. B: Environ.* 224 (2018) 660–670.
- [48] M. Laiq Ur Rehman, Q. Hou, X. Bai, Y. Nie, H. Qian, T. Xia, R. Lai, G. Yu, M. Ju, Regulating the alkalinity of carbon nitride by magnesium doping to boost the selective isomerization of glucose to fructose, *ACS Sustain. Chem. Eng.* 10 (2022) 1986–1993.
- [49] I. Delidovich, Recent progress in base-catalyzed isomerization of D-glucose into D-fructose, *Curr. Opin. Green Sustain. Chem.* 27 (2021), 100414.
- [50] I. Graça, D. Iruretagoyena, D. Chadwick, Glucose isomerisation into fructose over magnesium-impregnated NaY zeolite catalysts, *Appl. Catal. B: Environ.* 206 (2017) 434–443.
- [51] P. Drabo, M. Fischer, V. Toussaint, F. Flecken, R. Palkovits, I. Delidovich, What are the catalytically active species for aqueous-phase isomerization of D-glucose into D-fructose in the presence of alkaline earth metal (hydr)oxides? *J. Catal.* 402 (2021) 315–324.
- [52] X. Hai, S. Xi, S. Mitchell, K. Harrath, H. Xu, D.F. Akl, D. Kong, J. Li, Z. Li, T. Sun, H. Yang, Y. Cui, C. Su, X. Zhao, J. Li, J. Pérez-Ramírez, J. Lu, Scalable two-step annealing method for preparing ultra-high-density single-atom catalyst libraries, *Nat. Nanotechnol.* 17 (2022) 174–181.
- [53] X. Zhao, R. Fang, F. Wang, X. Kong, Y. Li, Atomic design of dual-metal hetero-single-atoms for high-efficiency synthesis of natural flavones, *Nat. Commun.* 13 (2022) 7873.
- [54] Y. Song, E. Ozdemir, S. Ramesh, A. Adishev, S. Subramanian, A. Harale, M. Albuali, B.A. Padhel, A. Jamal, D. Moon, S.H. Choi, C.T. Yavuz, Dry reforming of methane by stable Ni-Mo nanocatalysts on single-crystalline MgO, *Science* 367 (2020) 777–781.
- [55] Q. Zhang, S. Xu, Y. Cao, R. Ruan, J.H. Clark, C. Hu, D.C.W. Tsang, Sustainable production of gluconic acid and glucuronic acid via microwave-assisted glucose oxidation over low-cost Cu-biochar catalysts, *Green. Chem.* 24 (2022) 6657–6670.
- [56] Y. El-Sayed, T.J. Bandosz, Acetaldehyde adsorption on nitrogen-containing activated carbons, *Langmuir* 18 (2002) 3213–3218.
- [57] X. Ye, X. Shi, J. Li, B. Jin, J. Cheng, Z. Ren, H. Zhong, L. Chen, X. Liu, F. Jin, T. Wang, Fabrication of Mg-Al hydrotalcite/carbon nanotubes hybrid base catalysts for efficient production of fructose from glucose, *Chem. Eng. J.* 440 (2022), 135844.
- [58] S. Dutta, I.K.M. Yu, J. Fan, J.H. Clark, D.C.W. Tsang, Critical factors for levulinic acid production from starch-rich food waste: solvent effects, reaction pressure, and phase separation, *Green. Chem.*, (2021).
- [59] Y. Shao, D.-Y. Zhao, W. Lu, Y. Long, W. Zheng, J. Zhao, Z.-T. Hu, MgO/Carbon nanocomposites synthesized in molten salts for catalytic isomerization of glucose to fructose in aqueous media, *Green. Chem. Eng.* 3 (2022) 359–366.
- [60] N. Deshpande, L. Pattanaik, M.R. Whitaker, C.-T. Yang, L.-C. Lin, N.A. Brunelli, Selectively converting glucose to fructose using immobilized tertiary amines, *J. Catal.* 353 (2017) 205–210.
- [61] T. Zhu, F. Qu, B. Liu, H. Liang, The influence of environmental factor on the coagulation enhanced ultrafiltration of algae-laden water: Role of two anionic surfactants to the separation performance, *Chemosphere* 291 (2022), 132745.
- [62] X. Ye, X. Shi, B. Jin, H. Zhong, F. Jin, T. Wang, Natural mineral bentonite as catalyst for efficient isomerization of biomass-derived glucose to fructose in water, *Sci. Total Environ.* 778 (2021), 146276.
- [63] Q. Guo, L. Ren, P. Kumar, V.J. Cybulskis, K.A. Mkhyoyan, M.E. Davis, M. Tsapatsis, A chromium hydroxide/MIL-101(Cr) MOF composite catalyst and its use for the selective isomerization of glucose to fructose, *Angew. Chem. Int. Ed.* 57 (2018) 4926–4930.
- [64] C.G. Yoo, N. Li, M. Swannell, X. Pan, Isomerization of glucose to fructose catalyzed by lithium bromide in water, *Green. Chem.* 19 (2017) 4402–4411.
- [65] Y. Román-Leshkov, M. Moliner, J.A. Labinger, M.E. Davis, Mechanism of glucose isomerization using a solid Lewis acid catalyst in water, *Angew. Chem. Int. Ed.* 49 (2010) 8954–8957.